La mer 36: 43-55, 1998
Société franco-japonaise d'océanographie, Tokyo

Seasonal variation of three-dimensional circulations in the Gulf of Thailand

Tetsuo YANAGI* and Toshiyuki TAKAO**

Abstract: Seasonal variation of three-dimensional circulations in the Gulf of Thailand is investigated by diagnostic numerical calculation using the observed water temperature, salinity and wind data during NAGA cruises from October 1959 to August 1960. The wind-driven current dominated and the circulations were nearly barotropic in the Gulf of Thailand throughout the year. The clockwise circulation developed at the central part of the Gulf of Thailand both in the northeast and southwest monsoons.

1. Introduction

The Gulf of Thailand is situated in the southwestern part of the South China Sea and its averaged depth is about 40m (Fig. 1). The NAGA cruises were carried out to investigate the seasonal variation of water temperature and salinity distributions in the whole area of the Gulf of Thailand from October 1959 to August 1960 (Fig. 2, WYRTKI, 1961). The observed results were analysed in detail and the characteristics of seasonal variations in water temperature, salinity and density fields have been revealed (ROBINSON, 1961; WYRTKI, 1961). However the seasonal variation of three-dimensinal structure of water circulation in the Gulf of Thailand has not been elucidated yet.

POHLMAN (1987) conducted a three-dimensional numerical experiment in the whole area of the South China Sea including the Gulf of Thailand with the horizontal mesh size of 50 $\times$50 km and vertical 12 layers. He showed that the monsoon gave the largest effect to the seasonal variation of circulation in the Gulf of Thailand and a barotropic counterclockwise circulation developed in the Gulf of Thailand during boreal winter and a clockwise one during boreal summer by the monsoon. AZMY *et al.* (1991) calculated the horizontal two-dimensional wind-driven current in the Gulf of Thailand with fine mesh size of 20 km $\times$ 20 km under the uniform sea surface wind and concluded that a counterclockwise circulation dominated at the head of the Gulf and a clockwise one at the central part of the Gulf during boreal winter and a large clockwise one during the boreal summer.

In this paper, we conduct a diagnostic three-dimensional numerical calculation using the observed water temperature, salinity and wind data during the NAGA cruises from October 1959 to August 1960 in order to elucidate the seasonal variation of three-dimensional water circulation in the Gulf of Thailand.

2. Observed data

The observation stations of NAGA cruises cover the whole area of the Gulf of Thailand are shown in Fig. 2. The water temperature, salinity and sea surface wind are objectively interpolated on mesh points with the size of 10 km using the exponential function of Eq.(1) with the effective length of L =100 km.

$$T(x,y)=\frac{\sum_i \exp\left\{-\left(\frac{r_i}{L}\right)^2 T_i\right\}}{\sum_i \exp\left\{-\left(\frac{r_i}{L}\right)^2\right\}} \qquad (1)$$

where $T(x, y)$ denotes the interpolated value at the point (x, y), i the observation station, r_i the length between the interpolated point (x, y) and the observation station i and T_i the

* Research Institute for Applied Mechanics, Kyushu University, Kasuga 816, Japan
** Civil and Environmental Engineering, Ehime University, Matsuyama 790, Japan

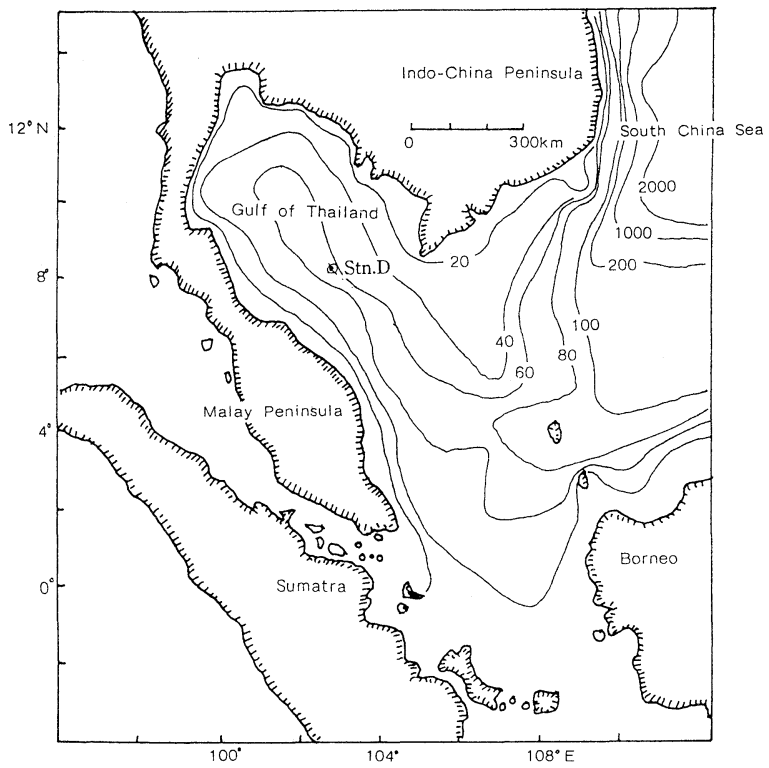

Fig. 1. The Gulf of Thailand. Numbers show the depth in meter and Stn. D is the deepest point in the Gulf (water depth is 83m).

observed value at station i.

The seasonal variation of interpolated horizontal distributions of water temperature, salinity and denstiy (sigma-t), which is calculated using the conventional nonlinear state eqution, 5 m below the sea surface is shown in Fig. 3. Surface water temperature is the highest during March to April 1960 because the solar radiation is the strongest in this season. Horizontal gradient of water temperature is very small except at the mouth of the Gulf during March to April 1960. Low salinity water mass spreads along the northeastern coast of the Gulf of Thailand in October 1959 and during June to August 1960. On the other hand, a remarkable salinity front develops at the mouth of the Gulf during December 1959 to January 1960 and during March to April 1960. The density field is similar to the salinity one and this means that the density distribution is mainly governed by the salinity distribution in the Gulf of Thailand. This fact suggests the the Gulf of Thailand has the characteristics of estuary.

The seasonal variation in vertical distributions of water temperature, salinity and density at the deepest position(Stn. D in Fig. 1) in the Gulf of Thailand is shown in Fig. 4. The stratification develops during March to August 1960, in the southwest monsoon season, and the water column is vertically well mixed during Octover 1959 to January 1960, in the northeast monsoon season.

The seasonal variation of the interpolated sea surface wind observed by researching vessels during the NAGA cruises is shown in Fig. 5. The northeast monsoon prevailed during October 1959 to January 1960 but the southwest monsoon during March to August 1960.

3. Diagnostic numerical calculation

The horizontal mesh size of numerical model is 10 km×10 km and the water colum is vertically divided into ten layers with the sigma-

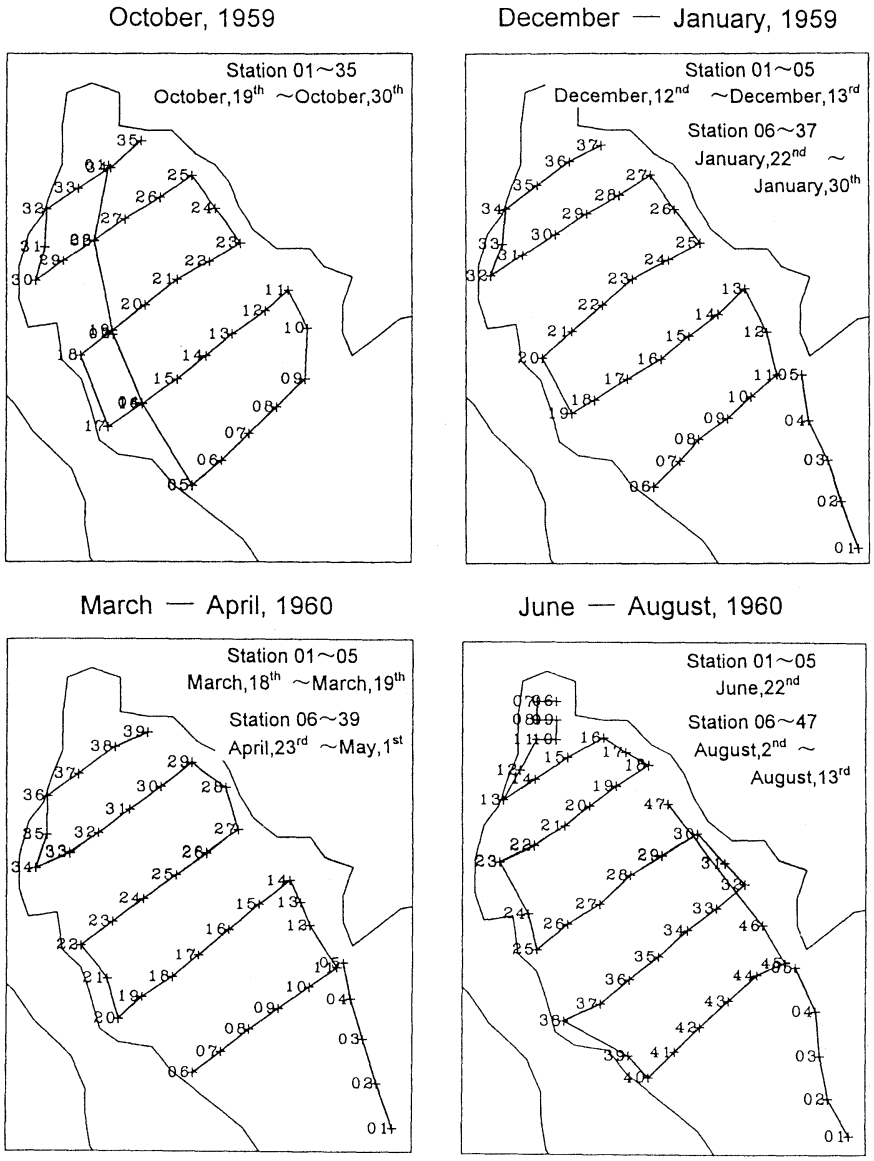

Fig. 2. Observation stations during the NAGA cruises.

coordinate. Using conventional notation, the governing equations under the cartesian coordinate are as follows

$$\frac{\partial U}{\partial t}+U\frac{\partial U}{\partial x}+V\frac{\partial U}{\partial y}+W\frac{\partial U}{\partial z}-fV$$

$$=-\frac{1}{\rho_0}\frac{\partial P}{\partial x}+\frac{\partial}{\partial x}(A_h\frac{\partial U}{\partial x})+\frac{\partial}{\partial y}(A_h\frac{\partial U}{\partial y}) \quad (2)$$

$$+\frac{\partial}{\partial z}(A_V\frac{\partial U}{\partial z})+T_x$$

$$\frac{\partial V}{\partial t}+U\frac{\partial V}{\partial x}+V\frac{\partial V}{\partial y}+W\frac{\partial V}{\partial z}+fU$$

$$=-\frac{1}{\rho_0}\frac{\partial P}{\partial y}+\frac{\partial}{\partial x}(A_h\frac{\partial V}{\partial x})+\frac{\partial}{\partial y}(A_h\frac{\partial V}{\partial y}) \quad (3)$$

$$+\frac{\partial}{\partial z}(A_V\frac{\partial V}{\partial z})+T_y$$

$$P=\rho_0 g\eta+\rho_0\int_0^z B\mathrm{d}z \quad (4)$$

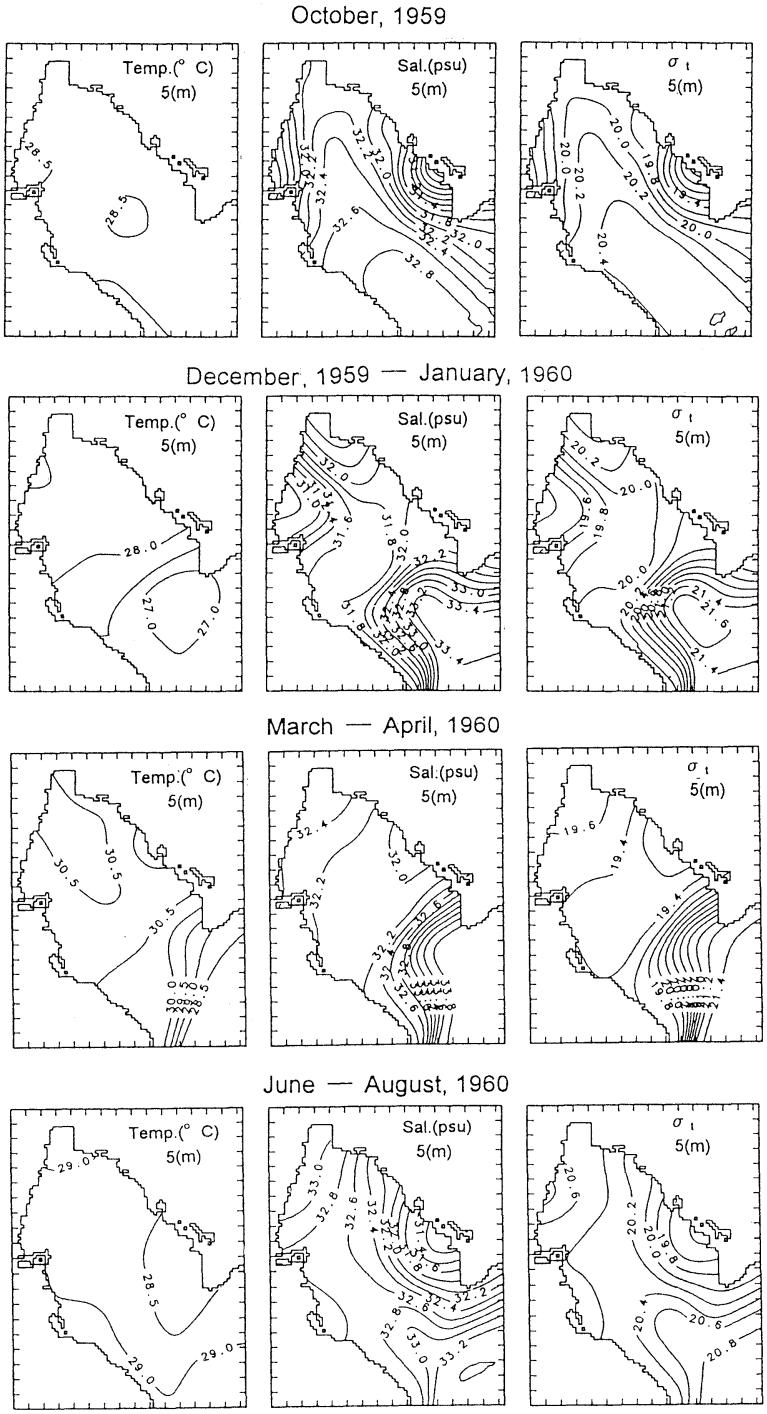

Fig. 3. Seasonal variation in horizontal distributions of interpolated water temperature, salinity and density 5 m below the sea surface in the Gulf of Thailand.

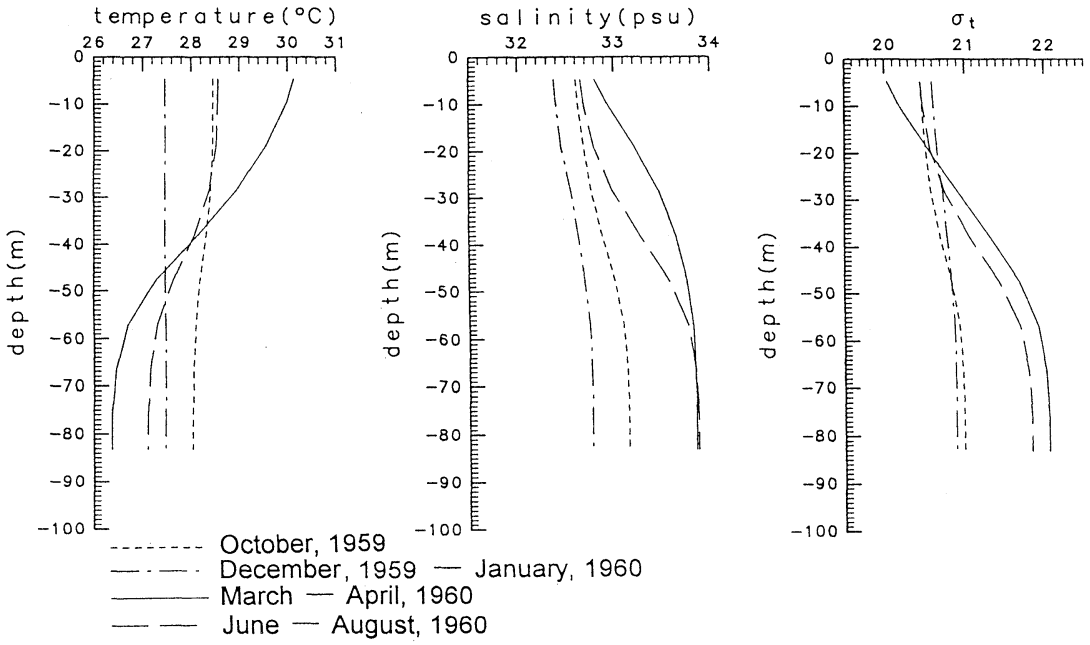

Fig. 4. Seasonal variation in vertical distributions of interpolated water temperature, salinity and density at the deepest position (Stn. D shown in Fig. 1) of the Gulf of Thailand.

$$B = \frac{\rho_0 - \rho}{\rho_0} \tag{5}$$

$$\frac{\partial U}{\partial x} + \frac{\partial V}{\partial y} + \frac{\partial W}{\partial z} = 0 \tag{6}$$

$$\frac{\partial T}{\partial t} + U\frac{\partial T}{\partial x} + V\frac{\partial T}{\partial y} + W\frac{\partial T}{\partial z} = \frac{\partial}{\partial x}\left(K_h \frac{\partial T}{\partial x}\right) + \frac{\partial}{\partial y}\left(K_h \frac{\partial T}{\partial y}\right) + \frac{\partial}{\partial z}\left(K_v \frac{\partial T}{\partial z}\right) + \gamma(T^* - T) \tag{7}$$

$$\frac{\partial S}{\partial t} + U\frac{\partial S}{\partial x} + V\frac{\partial S}{\partial y} + W\frac{\partial S}{\partial z} = \frac{\partial}{\partial x}\left(K_h \frac{\partial S}{\partial x}\right) + \frac{\partial}{\partial y}\left(K_h \frac{\partial S}{\partial y}\right) + \frac{\partial}{\partial z}\left(K_v \frac{\partial S}{\partial z}\right) + \gamma(S^* - S) \tag{8}$$

Here U, V and W are x (eastward), y (northward) and z (upward) components of residual flow, respectively, f is the Coriolis parameter, t is time, p is pressure, ρ is water density, ρ_0 is the reference density, g is the gravitational acceleration ($=980\text{cm}^2\,\text{s}^{-1}$), A_h ($=5\times10^6\text{cm}^2\,\text{s}^{-1}$) and K_h ($=5\times10^6\text{cm}^2\,\text{s}^{-1}$) are horizontal eddy viscosity and diffusivity, respectively. A_v ($=10\text{cm}^2\,\text{s}^{-1}$) and K_v ($=10\text{cm}^2\,\text{s}^{-1}$) is the vertical eddy viscosity and diffusivity, respectively. T_x and T_y denote x and y components of the tidal stress. T is water temperature and S is salinity. The density is calculated from T and S with use of the conventional nonlinear state equation.

The last terms in Eqs. (7) and (8) are called γ terms which are introduced by SARMIENT and BRYAN (1982) to prevent calculated values T and S from deviating greatly from observed values T^* and S^*. In other words, if there is an observed density that significantly deviates frome a local advective-diffusive balance, the density is smoothed by the model to satisfy the balance to some extent. The degree of modification is represented by γ. For small γ, the model is near to be independent of the data and approaches prognostic models. For large γ, the model is restricted by the data and approaches purely diagnostic model(FUJIO and IMASATO,

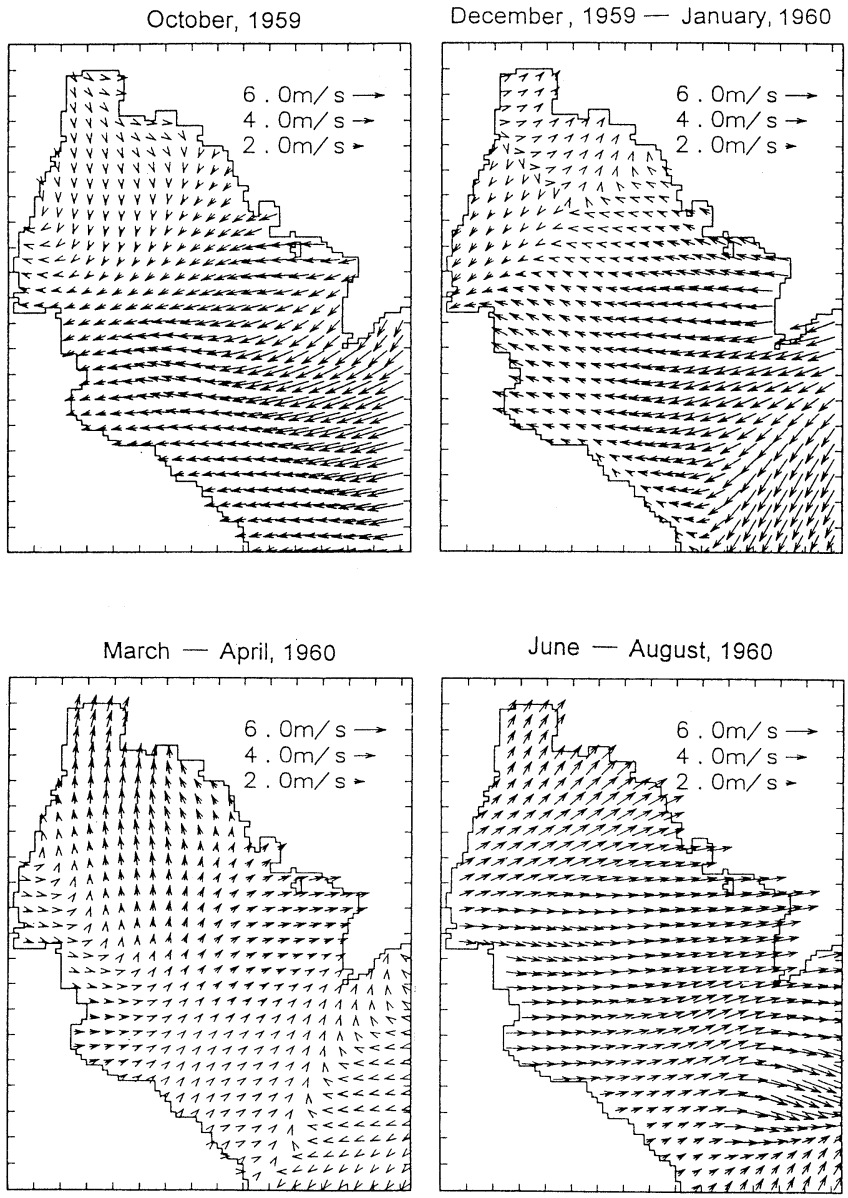

Fig. 5. Seasonal variation in interpolated sea surface wind observed by researching vessels during the NAGA cruises in the Gulf of Thailand.

1991). We prefer a larger γ because we intend to diagnose velocity field from hydrographic data, not to predict it. As long as we use a larger γ, the density deviates little from the observed values. Hence the derived velocity is almost independent of eddy diffusivity as discussed later. In this case, we use $\gamma = 1/12$ hours. The change of γ affected little to the calculated results in this numerical experiments.

T_x and T_x express the effect of the tidal stress to the residual flow field (averaged circulation over the tidal cycle) and is calculated using the following equations,

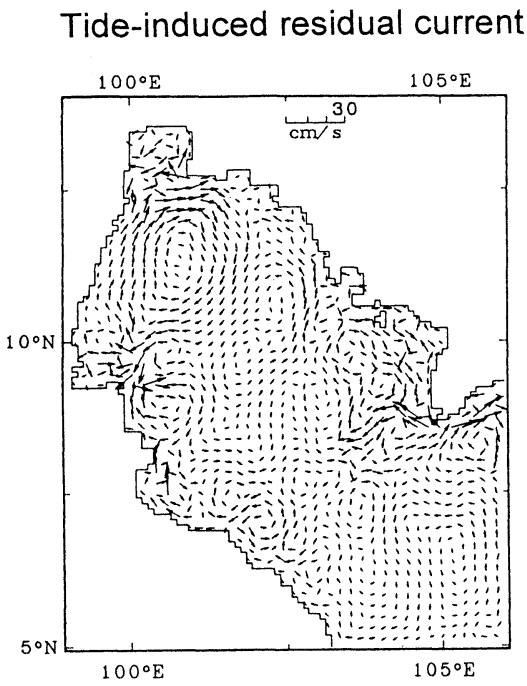

Fig. 6. Tide-induced residual current generated by 4 major tidal constituents (M_2, S_2, K_2 and O_1) in the Gulf of Thailand.

$$T_x = \left\{ u\frac{\partial u}{\partial x} + v\frac{\partial u}{\partial y} \right\}$$

$$T_y = \left\{ u\frac{\partial v}{\partial x} + v\frac{\partial v}{\partial y} \right\} \qquad (9)$$

Here u and v denote the tidal current components in x and y direction, respectively and { } the average during one-tidal cycle. Tidal currents of 4 major constituents (M_2, S_2, K_1 and O_1) are already calculated in the Gulf of Thailand (YANAGI and TAKAO, 1998) and the tide-induced residual current generated only by the tidal stress of 4 major constituents is shown in Fig. 6. A clockwise residual circulation with the speed of about 5 cm s^{-1} is induced near the head of the Gulf of Thailand and many eddies are generated in the whole area of the Gulf.

The boundary condition for momentum is no-slip condition at the lateral wall. The bottom stress (τ_x^b, τ_y^b) is given as follows,

$$\rho_0\left(A_v\frac{\partial U}{\partial z},\ A_v\frac{\partial V}{\partial z} \right) = (\tau_x^b,\ \tau_y^b) \qquad (10)$$

$$(\tau_x^b, \tau_y^b) = \rho_0\gamma_b^2(U\sqrt{U^2+V^2}, V\sqrt{U^2+V^2}) \qquad (11)$$

where $\gamma_b^2 = 0.0026$) is the bottom drag coefficient.

The sea surface is assumed to be free-surface, and the sea surface drag force(τ_x^s, τ_y^s) is given by

$$\rho_0\left(A_v\frac{\partial U}{\partial z},\ A_v\frac{\partial V}{\partial z} \right) = (\tau_x^s,\ \tau_y^s) \qquad (12)$$

$$(\tau_x^s, \tau_y^s) = \rho_a C_a\left(W_x\sqrt{W_x^2+W_y^2}, W_y\sqrt{W_x^2+W_y^2} \right) \qquad (13)$$

where ρ_a ($=0.0012$ g cm^{-3}) is the air density, C_a ($=0.0013$) the sea surface drag coefficient and W_x and W_y the wind velocity in x and y directions, respectively.

The boundary condition for water temperature and salinity is a no-flux condition at the lateral wall, at the bottom, and at the sea surface. We cannot give the approapriate inflow and outflow conditions across the mouth of the Gulf of Thailand because we have no observed data on the water exchange between the Gulf of Thailand and the South China Sea. Therefore the radiation condition is adopted for the sea surface gradient and velocity along the open boundary of this model.

The leap-frog scheme with use of Dufort-Frankel method is adopted for the temporal acceleration term, viscosity term and diffusive term and the Euler-Backward scheme is inserted every ten time steps (the time step is 120 seconds). The central difference scheme is adopted for the advection term and the semi-implicit scheme is used for the calculation of water elevation (BACKHAUS, 1983).

We conducted several other numerical experiments by changing the magnitude of horizontal and vertical viscosity and diffusivity but the calculated results did not change except the small change of the speed of residual flow.

4. Results

The calculated results on the seasonal variation in circulations at the three depths are shown in Fig. 7. A clockwise circulation and a counterclockwise one developed from the surface to the bottom at the central part and at the mouth of the Gulf of Thailand, respectively, in October 1959. Such circulation pattern did not

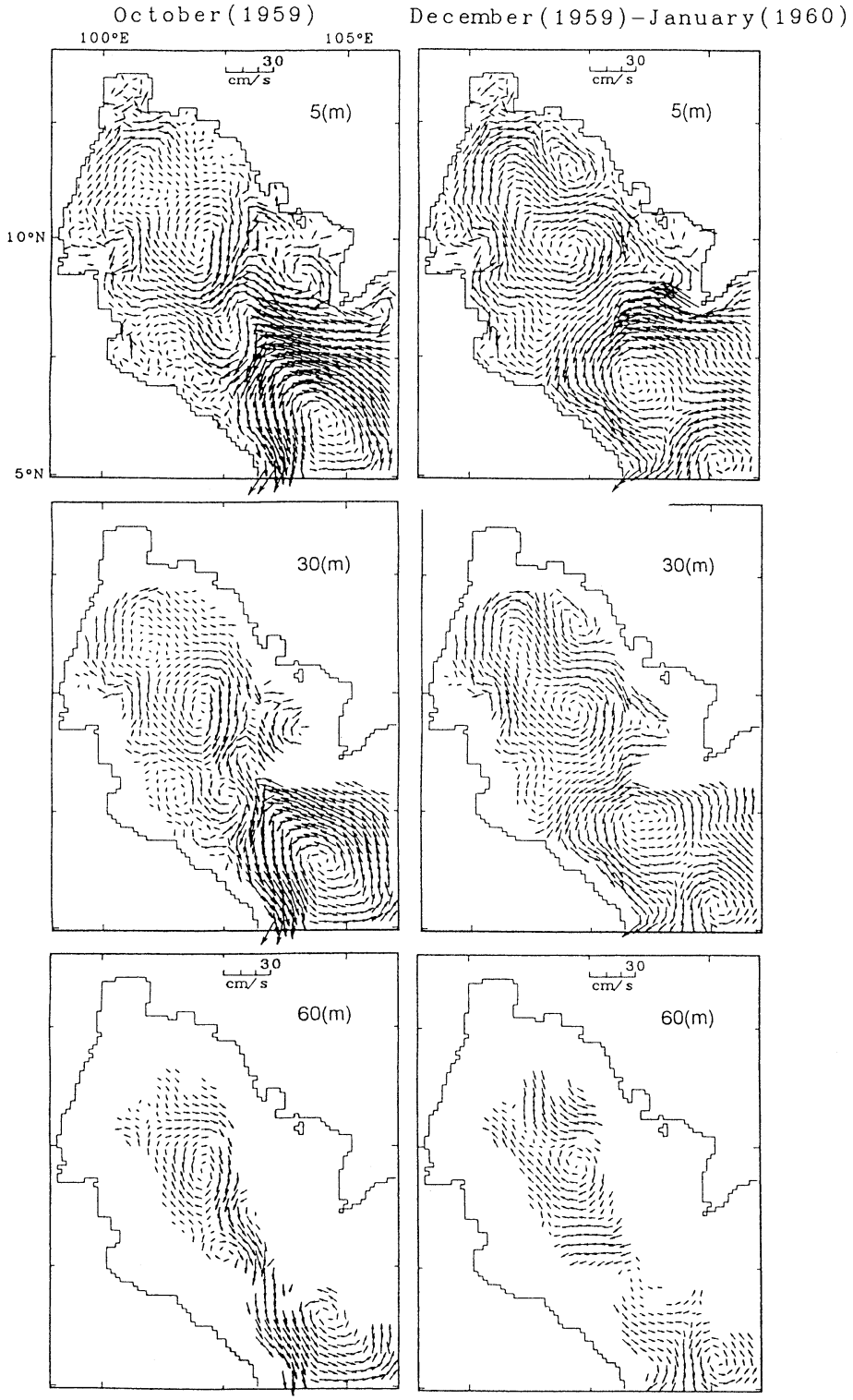

Fig. 7. Seasonal variation of circulations 5 m, 30 m and 60 m below the sea surface in the Gulf of Thailand.

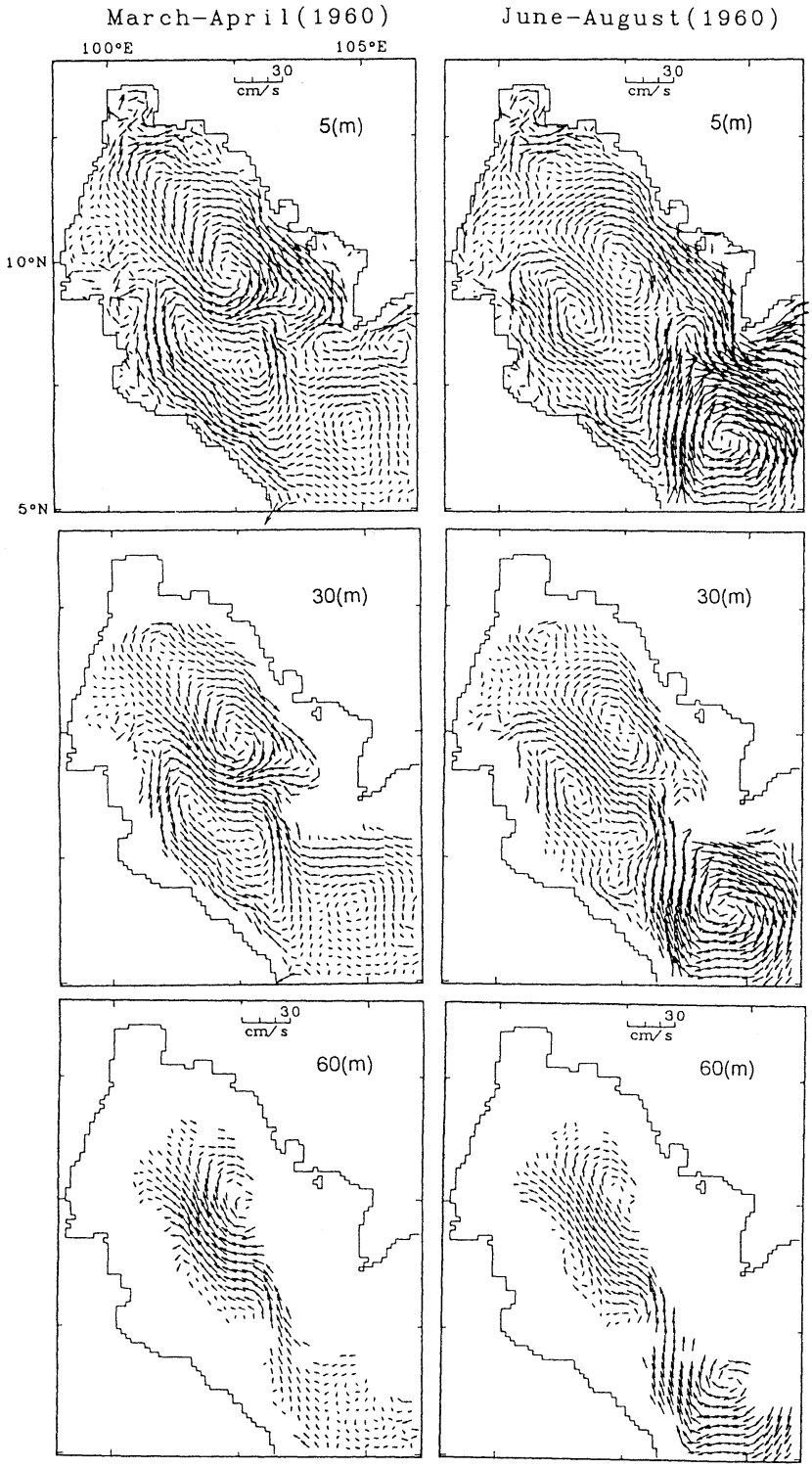

Fig. 7(continued)

change except the weaker current speed during December 1959 to January 1960. A clockwise circulation and a counterclockwise on developed from the surface to the bottom in the northern and southern parts of the Gulf, respectively, during March to April 1960. Such circulation pattern did not change except the addition of a strong clockwise circulation at the mouth of the Gulf during June to August 1960.

The observed data of residual flow (averaged flow over tidal period) in the Gulf of Thailand are very limited. The cmparison of observed residual flows at 7 stations in March 1961 (ROBINSON, 1974) and calculated ones at the corresponding stations during March to April 1960 are shown in Fig. 8. In current measurements during March 1961, the Roberts Current Meters was lowered on the hour, starting just below the sea surface and continuing at various intervals to the bottom at each station. A complete lowering was made in an approximately twenty minutes. The observed values were considered average for that hours and the averaged value during 26 to 29 hours were calculated to obtain the residual flow at each station (ROBINSON, 1974). In Fig. 8, the thin full lines show the observed residual flows at various depths of each station and the thick full line the averaged sea surface wind during the current measrement. The broken lines in Fig. 8 show the calculated ones at the corresponding stations in our calculation.

The observed residual flows in March 1961 shows principally the barotropic strcture except Stas. 2 and 6 and such a characteristic of observed residual flows is well reproduced by our numerical experiment as shown in Fig. 8. The dominance of barotropic structure of residual flows even in the most stratified season of March, as shown in Fig. 4, suggests that the residual flows in the Gulf of Thailand show the barotropic characteristic throughout the year as shown in Fig. 7.

Roughly speaking, the calculated residual flows and observed ones coincide at Sta. 1 except a discrepancy of the current direction in the deep part. The calculated residual flows at Sta. 2 coincide with observed ones excpet a discrepancy of current direction in the surface layer. The calculated direction of residual flow at Sta. 3 coincide with the observed one though its speed is much smaller than that of observed one. The calculated speed of residual flow at Sta. 4 is much smaller than the observed one, perhaps due to the weaker wind speed during March to April 1961 than that in March 1960. The calculated residual flows at Stas. 5, 6 and 7 do not coincide with the observed ones, perhaps due to the different wind direction and speed in both periods.

5. Discussion

The circulation pattern in October 1959 and that during December 1959 to January 1960 are very similar as shown in Fig. 7 though the horizontal density distributions in both periods are different as shown in Fig. 3. On the other hand, the sea surface wind patterns in both periods are very similar as shown in Fig. 5, that is, the northeast monsoon prevails. These facts suggest that the main component of residual flow in the Gulf of Thailand during the northeast monsoon is the wind-driven current.

The residual flow patterns during March to April 1960 and during June to August 1960 are also similar except those at the mouth of the Gulf as shown in Fig. 7. The southwest monsoon prevailed in the Gulf during both periods but the sea surface wind patterns were different only at the mouth of the Gulf as shown in Fig. 5. These facts also suggest that the main component of residual flow in the Gulf of Thailand during the southwest monsoon is the wind-driven current.

Uisng a baroclinic three-dimensional prognostic model, POHLMAN (1987) showed that the dominance of barotropic circulations in the Gulf of Thailand during both northeast and southwest monsoons. However, a counterclockwise circulation developed during the northwest monsoon and clockwise one during the southwest monsoon from his calculated results.

It is very interesting to note that the similar clockwise circulations are induced at the central part of the Gulf under the opposite sea surface wind patterns during the northeast and southwest monsoons as shown in Figs. 5 and 7 by our calculation results. One of the reasons of discrepancy between our results and those by

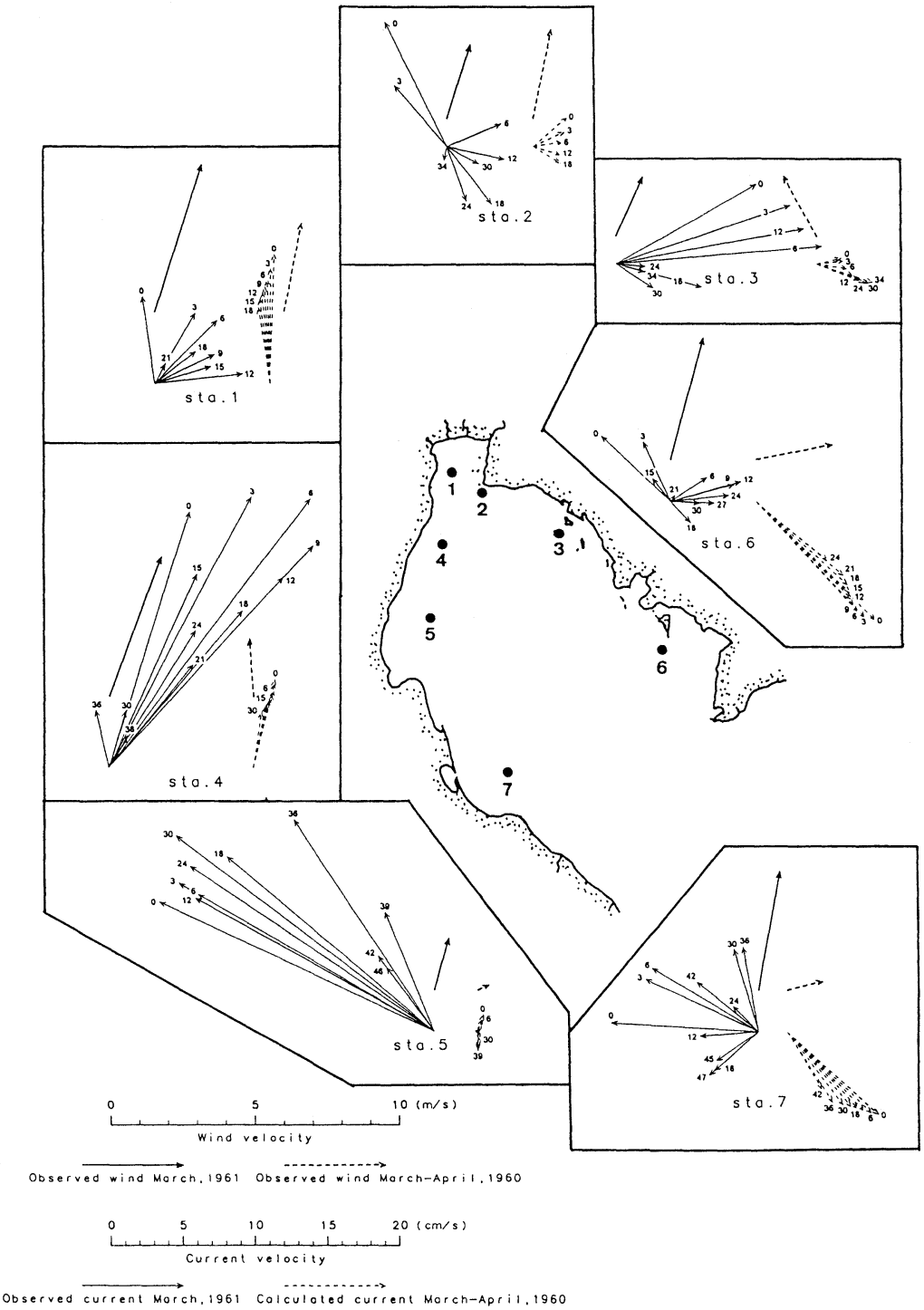

Fig. 8. Comparison of observed wind and residual flow in March 1961 and the calculated ones in March–April 1960 in the Gulf of Thailand. Numbers show the observation depth in meters.

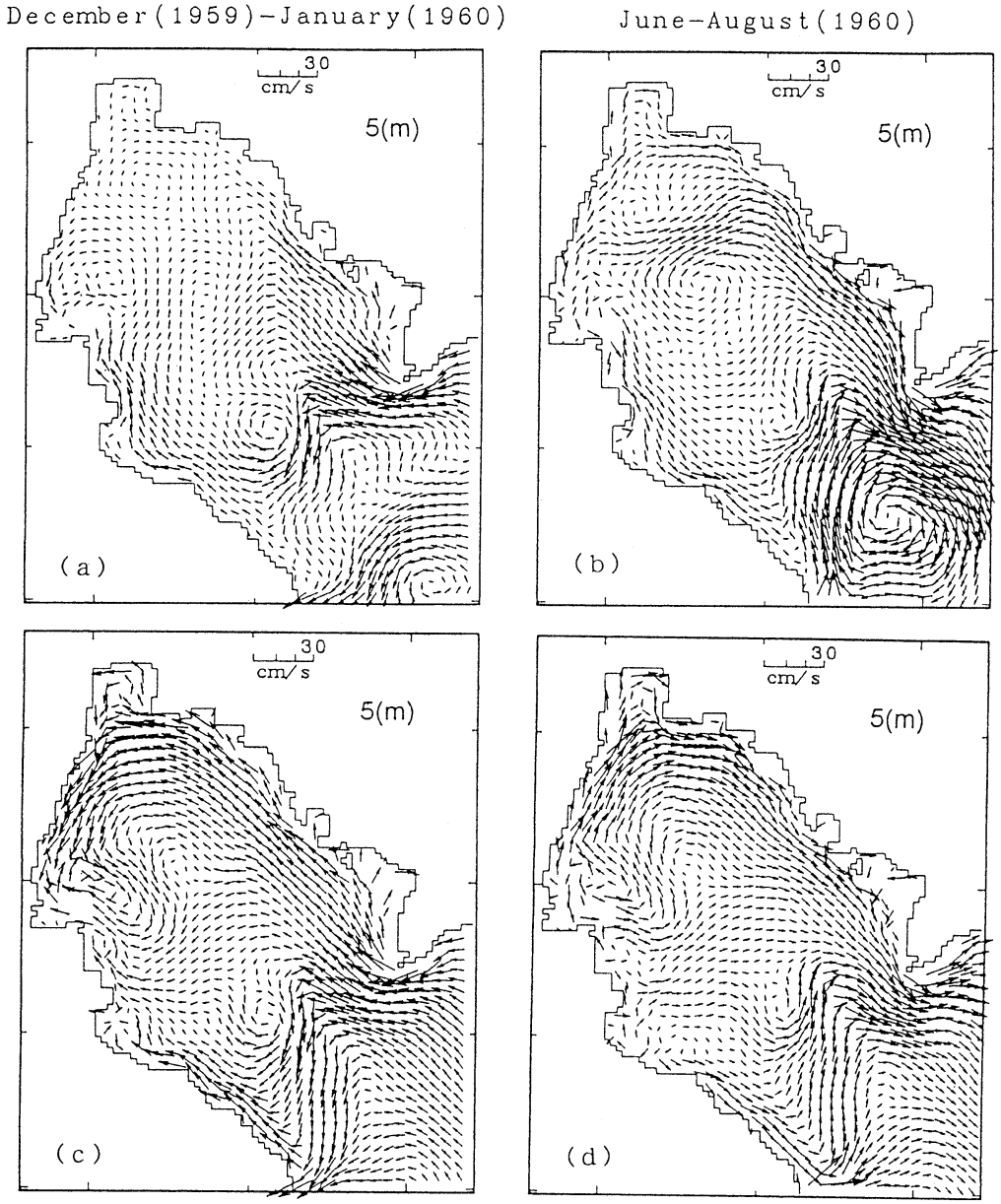

Fig. 9. Residual flow in the uniform density field under the observed sea surface wind during December 1959 to January 1960 (a), during June to August 1960 (b), that under the averaged uniform sea surface wind during December 1959 to January 1960 (c) and during June to August 1960 (d).

POHLMAN (1987) may be the difference of the mesh size of the used numerical model, that is, the horizontal mesh size of our numerical model is 10km×10km though that of POHLMAN (1987) is about 50km×50km. Another reason of the discrepancy between both calculated results may be the difference of the sea surface wind patterns in both models. The horizontal gradient of sea surface wind vectors is rather large in our model as shown in Fig. 5 because they are snap shot results during the field observations though the horizontal gradient of

sea surface wind vectors in POHLMAN (1987) is very small because he used the climatological mean of sea surface wind compiled by HELLERMAN (1968).

We conduct other numerical experiments on the residual flow in the uniform density field using the same governing equations from Eqs. (2) to (13) including the tidal stress. The calculated wind-driven and tide-induced residual current 5 m below the sea surface under the observed sea surface wind shown in Fig. 5 during December 1959 to January 1960 are shown in Fig. 9 (a) and those during June to August in Fig. 9 (b). Both results are similar to the calculated ones including the observed density field shown in Fig. 7 except the weaker current speed. This fact suggests that the basic patterns of residual flow in the Gulf of Thailand is determined by the monsoon and the tidal stress. The density field strengths the current speed of residual flow.

Lastly we conduct numerical experiments on the residual flow in the uniform density field using the same governing equations from Eqs.(2) to (13) including the tidal stress under the uniform sea surface wind, which is obtained by averaging the observed sea surface wind over the Gulf of Thailand; the east-northeast wind with the speed of 5.5m s^{-1} during December 1959 to January 1960 and the westsouthwest wind with the speed of 5.1m s^{-1} during June to August 1960. The results are shown in Fig. 9 (c) and (d). The result shown in Fig. 9 (d) during June to August 1960 is similar to that under the observed sea surface wind field shown in Fig. 9 (b). However the residual flow under the uniform sea surface wind during December 1959 to January 1960 shown in Fig. 9 (c) is drastically changed from that under the observed sea surface wind shown in Fig. 9 (a), that is, the counterclockwise circulation develops at the central part of the Gulf in Fig. 9 (c) instead of the clockwise circulation in Fig. 9 (a). This fact suggests that the wind stress curl is very important to the residual flow field in the Gulf of Thailand, that is, the clockwise circulation at the central part of the Gulf during the northeast monsoon is generated by the negative vorticity of the sea surface wind at this time.

The results of this study suggest that the sea surface wind curl plays a very important role in the determination of residual flow pattern in the Gulf of Thailand. Therefore we have to elucidate the detailed horizontal distribution of sea surface wind over the Gulf of Thailand for the study of water circulation in the Gulf.

Acknowledgements

The authors express their sincere thanks to Prof. C. GARRET of the University of Victoria, Canada who kindly supplys the data file of NAGA cruises and Dr. A. Isobe of Kyushu University for his fruitful discussion. This study was partly supported by the research fund from the Ministry of Education, Science and Culture, Japan.

References

AZMY, A, R., Y. ISODA and T. YANAGI (1991): Sea level variation due to wind around West Malaysia. Memoirs of the Faculty of Engineering, Ehime University, 12-2, 143-156.

BACKHAUS, J. O. (1983): A semi-implicit scheme for the shallow water equation for application to shelf water sea modeling. Continental Shelf Res., **2**, 243-254.

FUJIO, S. and N. IMASATO (1991): Diagnostic calculation for circulation and water mass movement in the deep Pacific. J. Geophys. Res., **96**, 759-774.

HELLERMAN, S. (1968): An update estimate of the wind stress on the world ocean. Monthly Weather Review, **96**.

POHLMAN, T. (1987): A three-dimenional circulation model of the South China Sea. *In* "Three-dimensional models of marine and estuarine dynamics", ed. by NIHOUL, J. J. and B. M. JAMART, Elsevier, New York, 245-268.

ROBINSON, M. K. (1961): The physical oceanography of the Gulf of Thailand, Naga Expedition. Naga Report Volume 3, Part 1, Scripps Institution of Oceanography, La Jolla, California, 5-110.

SARMIENTO, J. J. and K. BRYAN (1982): A ocean transport model for the North Atlantic. J. Geophys. Res., **87**, 394-408.

WYRTKI , K. (1961): Physical oceanography of the Southeast Asian waters. NAGA Report Volume 2, Scripps Institution of Oceangraphy, La Jolla, California. 1-195.

YANAGI , T. and T. TAKANO (1998): A numerical simulation of tides and tidal currents in the South China Sea. Acta Oceanographic Taiwania (in press)

Received April 8, 1998
Accepted May 10, 1998